

Shear-thickening behaviour of concentrated polymer dispersions under steady and oscillatory shear

Li Chang · Klaus Friedrich · Alois K. Schlarb ·
Roger Tanner · Lin Ye

Received: 22 June 2010/Accepted: 3 August 2010/Published online: 13 August 2010
© Springer Science+Business Media, LLC 2010

Abstract The rheological behaviour of a 58 vol.% dispersion of styrene/acrylate particles in ethylene glycol was investigated using a plate-on-plate rheometer. Experimental results showed that the concentrated polymer dispersion exhibited a strong shear-thickening transition under both steady shear and dynamic oscillatory conditions. The low-frequency dynamic oscillatory behaviour could be reasonably interpreted in terms of the steady shear behaviour. Accordingly, the critical dynamic shear rate $\dot{\gamma}_{c,d}$, agreed well with the critical shear rate obtained in steady flow $\dot{\gamma}_{c,s}$, where $\dot{\gamma}_{c,d}$ was calculated as the maximum shear rate by the critical dynamic shear strain γ_c and the frequency ω , i.e. $\dot{\gamma}_{c,d} = \omega\gamma_c$. However, during high-frequency dynamic oscillation, it was observed that the shear thickening occurred only when an apparent critical shear strain was reached, which could not be fully explained by the wall-slipping effect. Based on freeze fracture microscopic observations, the effect of the micro-sized flocculation of particles on the rheology of concentrated dispersions was also discussed.

Introduction

Shear thickening is a non-Newtonian flow behaviour sometimes observed in highly concentrated dispersion systems [1–6], which could exhibit a reversible viscosity increase by several orders of magnitude with increasing shear rate (cf. Fig. 1) (often, in many polymer systems, the viscosity reduces as the shear rate rises). Initial interest in shear thickening arose from its association with damage to processing equipment and dramatic changes in suspension microstructures, resulting in poor fluid and coating properties. Nevertheless, possibilities to utilize such a unique system have recently come into consideration. With a highly nonlinear behaviour, shear-thickening fluids can provide self-limiting maximum rates of flow, which has been exploited in the design of damping, control devices, and “liquid armour”, etc. [7–9].

Due to its immense importance in industry, shear thickening in concentrated dispersions has attracted considerable interest during the last few decades. In particular, a number of studies focused on the dynamic oscillatory rheology of colloid suspensions [10], which is of practical concern for the development of engineering applications, e.g. damping devices based on the shear-thickening response. From a literature review, it is known that dynamic shear thickening occurs when an apparent critical strain is reached, which decreases with increasing frequency, but is eventually stable at higher frequencies [4, 5, 11, 12]. The shear thickening under low-frequency conditions was commonly interpreted by the steady shear behaviour. In particular, it is reported that the low-frequency strain-thickening data for the complex viscosity η^* as a function of the maximum dynamic shear-rate (obtained from the strain amplitude γ and the frequency ω) could be superposed against shear-thickening data for the

L. Chang (✉) · R. Tanner · L. Ye
School of Aerospace, Mechanical & Mechatronic Engineering,
The University of Sydney, Sydney, NSW 2006, Australia
e-mail: li.chang@sydney.edu.au

K. Friedrich
Institute for Composite Materials, University of Kaiserslautern,
67663 Kaiserslautern, Germany

A. K. Schlarb
Department of Mechanical and Process Engineering,
University of Kaiserslautern, 67663 Kaiserslautern, Germany

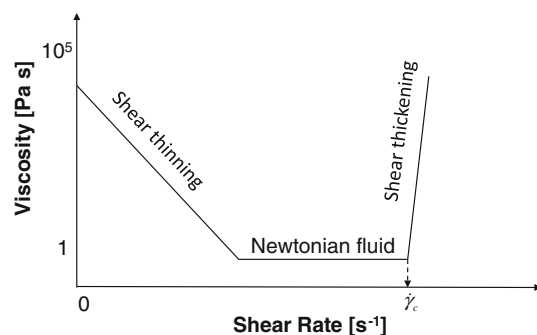


Fig. 1 Schematic illustration of the rheological behaviour of concentrated suspensions, showing the transition from shear thinning and/or Newtonian flow to shear thickening at a critical shear rate $\dot{\gamma}_c$. Measurements were made according to the data given in Refs. [2, 4–6]

steady viscosity η as a function of the steady shear rate $\dot{\gamma}_s$, i.e. $\eta * (\omega\gamma) = \eta(\dot{\gamma}_s)$. Such correlation was also called as a modified version of the Cox-Merz rule, due to its resemblance to the original Cox-Merz rule, $\eta * (\omega) = \eta(\dot{\gamma}_s)$ [4, 11]. The agreement between steady shear and low-frequency dynamic oscillatory response was also well supported by optical measurements on hard-sphere dispersions [13]. On the other hand, however, the underlying mechanism of the observed high-frequency limiting critical strain is still unclear. Some researchers suggested that a critical shear strain is necessary to cause dispersions to switch to the thickening state [4, 12]; whereas others considered that the minimum critical strain is an artefact of wall slipping [5].

In parallel to the arguments regarding the dynamic shear-thickening phenomenon, the basic mechanism of shear thickening is also under debate. Up to now, various models have been developed accounting for the origin of the shear-thickening behaviour in concentrated dispersions. For instance, in pioneering works, Hoffman [1, 2] proposed that the occurrence of shear thickening in dispersions resulted from a transition of an easy flowing state (where the particles are ordered in layers) to a disordered state, called “order-disorder” transition. However, it has been argued by subsequent researchers that it is not at all necessary to assume the existence of an ordered state before the shear-thickening transition. With the Stokesian dynamics simulations, Bossis and Brady [14] and Boersma et al. [15] indicated that shear thickening is caused by hydrodynamic lubrication forces between particles, resulting in the formation of a nonequilibrium, self-organized microstructure that develops under strong flows, denoted as “hydroclusters”. The simulations have shown that the Brownian contribution to the viscosity of hard sphere suspensions disappears at high shear rates (high Peclet numbers), whereas the hydrodynamic contribution remains largely constant prior to the shear-thickening regime.

Further experimental evidence for hydroclusters was provided by the rheo-optical and stress-jump measurements [13, 16, 17]. More recently, the model of “jamming transition” was also introduced in the field. It was indicated that shear thickening is the consequence of jammed particles due to the confinement [6, 18, 19]. Accordingly, positive normal forces were observed in the regime of shear thickening [6]. This is apparently in contrast to the negative normal stress as derived from hydrodynamic mechanisms [20, 21]. Despite the diversities among existing models, there is agreement in the shear-thickening mechanism for concentrated dispersions, i.e. that the macroscopic properties of dispersions are determined by the spatial organization of the particles, usually referred to as “microstructure”. Therefore, it is desirable to visualize the microstructure of shear-thickening fluids. However, due to the extremely high volume content and small size of dispersed particles, the direct observation of such microstructure still remains a challenge.

Although a significant number of experimental and theoretical studies have been made, the mechanism of shear thickening, particularly under high-frequency oscillatory motion, has not been fully understood. In this study, the steady and transient shear-thickening behaviours of concentrated polymer dispersions were systematically studied with different gap distances. The microstructure of the dispersions was examined by using freeze fracture microscopy. This study aims at a better understanding of the microstructure-related shear thickening in concentrated dispersions, as well as to determine whether the amplitude scale is required for the onset of a shear-thickening response. Such understanding is essential for the development of engineering devices utilizing the unique shear-thickening response.

Material and experimental

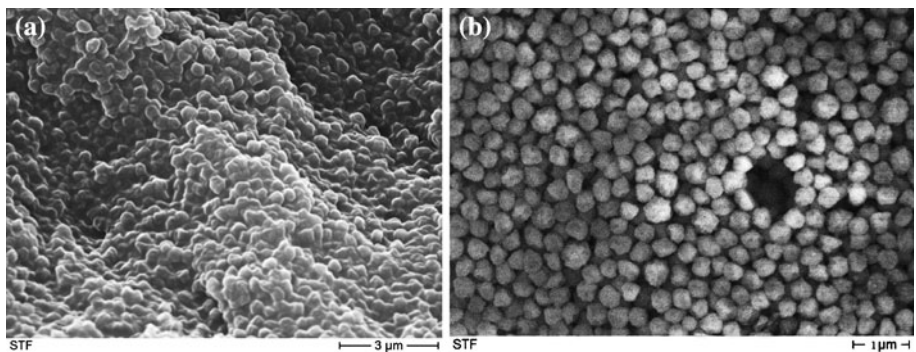
Material

The material used is a 58 vol.% dispersion of styrene/acrylate particles in ethylene glycol, supplied by BASF AG (Germany). Figure 2a shows the as-received material imaged by scanning electron microscopy (SEM). Figure 2b shows individual particles after water rinsing and drying. As shown in the figure, the shape of particles is irregular with an average size of ~ 300 nm.

Freeze fracture microscopy

Due to a very high particle concentration, it is difficult to directly identify the organization of particles with common microscopic techniques such as SEM (cf. Fig. 2a).

Fig. 2 SEM images of **a** the as-received polymer dispersions and **b** particles after water rinsing and drying



Therefore, freeze fracture microscopy was used to observe the inside distribution of particles in the matrix. The sample was prepared by freezing a droplet of the as-received material with liquid nitrogen. The fracture surface of the frozen sample was then replicated by evaporation of a platinum layer. Thereafter, the replica layer was cleaned by water. The dissolvable ethylene glycol was easily washed away, but most particles remained (got stuck) on the replica layer. The spatial distribution of particles was finally examined with a transmission electron microscope, Zeiss 902. The result is shown in Fig. 3. It is clear that most of particles are well dispersed, but micro-sized flocculation of particles is also noticed.

Rheological tests

Rheological tests were carried out on a rheometer (ARES rheometer, Rheometric Scientific) in both steady and dynamic modes at room temperature. A plate-on-plate geometry was used, with a plate diameter of 40 mm, as

shown in Fig. 4. The steady shear tests were conducted by stress-controlled shear rate sweep, whereas the dynamic oscillatory tests were performed by a strain sweep at constant frequency. To explore the effect of the gap distance, the rheological tests were conducted with various gaps: 50, 100, 200, 400 and 800 μm .

Results and discussion

Steady shear thickening

The principle shear-thickening effect of the fluid used in this study can be simply demonstrated by tearing a wooden stick out of the fluid at different speeds (Fig. 5). Using a speed of approximately 1 m/min allows to remove the stick from the liquid containing glass bowl, whereas a speed of about 1 m/s causes the liquid to behave in a solid fashion, so that the glass bowl with the “frozen” liquid is lifted up from the ground.

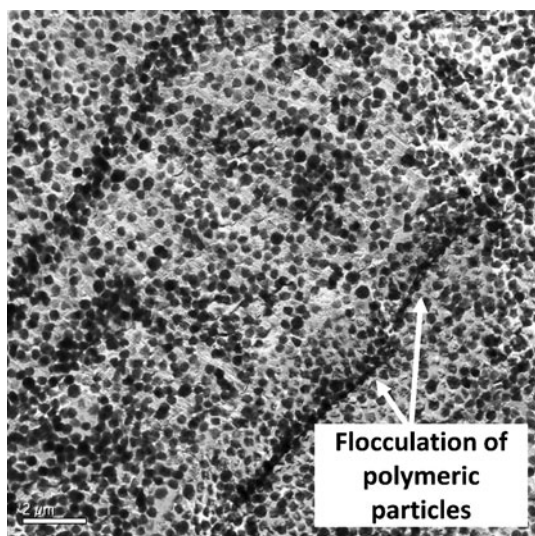


Fig. 3 TEM of the replica layer of the freeze fracture surface of polymer dispersions

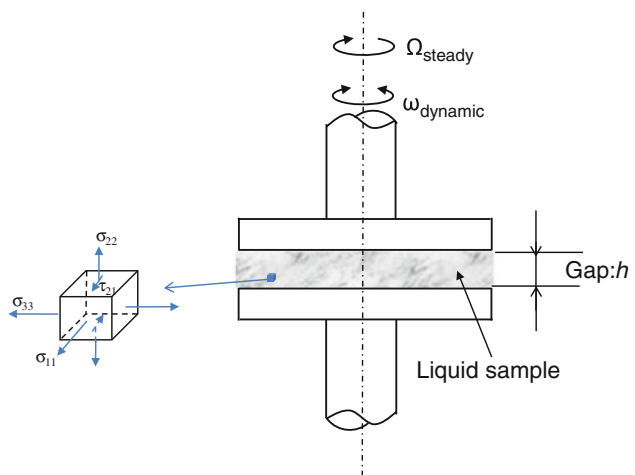


Fig. 4 A schematic diagram of the plate-on-plate rheometer with a gap size of h . The steady shear tests were conducted with increasing angular velocity, e.g. Ω_{steady} , whereas the dynamic tests were performed by a strain sweep at constant oscillatory frequency, e.g. ω_{dynamic} . The inserted cubic element shows the state of stresses generated for a simple flow

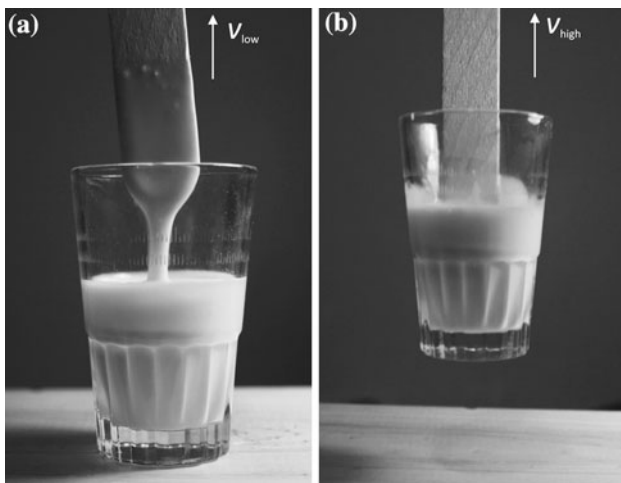


Fig. 5 Photos of the experiment of removing a stick out of the STF at **a** low and **b** high speed

Figure 6 shows the rheological behaviour of the polymer dispersion under steady shear, tested at different gap sizes. In all experiments, the tests were automatically stopped once the shear stress exceeded the maximum allowable torque moment of the rheometer, as a result of the strong shear-thickening effect.

The critical shear rate tends to decrease with an increase in the gap size, which can be explained by the wall slip of the liquid [5, 12]. It is suggested that the measured strain γ_m is the sum of the real strain γ_r and the artefact strain γ_s caused by the total slip distance D_s between the sample and the plates. Since $\gamma_s = D_s/h$ (where h is the gap size between the parallel plates), the measured strain is [5, 12]

$$\gamma_m = \gamma_r + D_s/h \quad (1)$$

Hence, the measured strain and accordingly the shear rate are geometry dependent, i.e. they are overestimated with

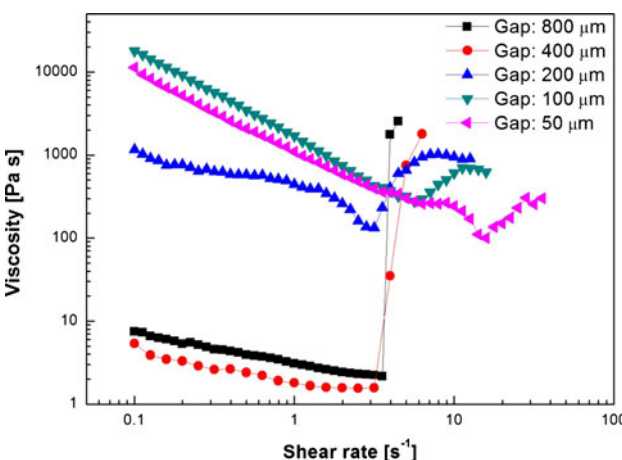


Fig. 6 Steady shear-thickening behaviour of the polymer suspension at different gap sizes

smaller gap sizes, but become more stable when the gap size is larger (cf. Fig. 6).

From Fig. 6, it is also noticed that the viscosity of the material measured with smaller gaps is clearly higher than the measured one at larger gap size. Moreover, with smaller gaps, the material shows obvious shear thinning at lower shear rates and then shear thickening at higher shear rates. The shear-thinning behaviour, also called thixotropy, is commonly encountered in flocculated gels, i.e. a step-wise increase in shear rate results in a time-dependent decrease in the viscosity as the material is broken down in the flow [3]. In our case, the shear thinning might also be caused by the flocculation of particles, which has been observed with freeze fracture microscopy (Fig. 3). When the gap size is relatively small, the randomly flocculated particles can build-up a bridge with each other and thus block the flow of liquid matrix. As a result, the initially measured viscosity is apparently high. During the steady shear under lower shear rates, the viscosity decreases because of the breakage of the linked flocculations and a subsequent formation of flowing layers. Shear thickening occurs when the critical shear rate is reached; here the hydrodynamic force dominates the interactions between particles [14, 15]. However, when the gap between the plates is large enough, the micro-sized flocculation cannot fully link the plates and therefore it does not contribute remarkably to the flow behaviour of the sample. As a result, the viscosity is rather low and stable at the low shear rates regime.

Shear thickening under dynamic oscillation

Figures 7 and 8 show the dynamic rheological properties of the material, compared to the steady shear-thickening behaviour tested with a gap size of 50 and 800 μm, respectively. Again, strong shear thickening effects were observed under all the test conditions, resulting in an automatic stop of the instrument.

According to the modified Cox–Merz rule [4, 11], the steady and complex viscosities should overlap, when plotted against the equivalent shear rates. However, such a relationship was not observed for our data. In particular, the viscosities measured with smaller gaps showed little repeatability and nonlinearity (Fig. 7). Despite apparent changes in the measured values of the viscosity, it can be noticed that there are two regimes of the dynamic shear-thickening behaviour, regardless of the size of the gaps (Fig. 9a). The first one represents the low-frequency regime, where the critical dynamic shear rate is stable and agrees well with the steady shear rate at the onset of shear thickening. The second one is the high-frequency regime, where the critical dynamic shear rate increases proportionally with the increase in frequency. Such two regimes

Fig. 7 **a** The dynamic rheological behaviour compared with the steady shear behaviour, using a gap size of 50 μm . **b** Elastic G' and viscous G'' moduli as a function of the dynamic shear rate at a constant frequency of 1 rad/s

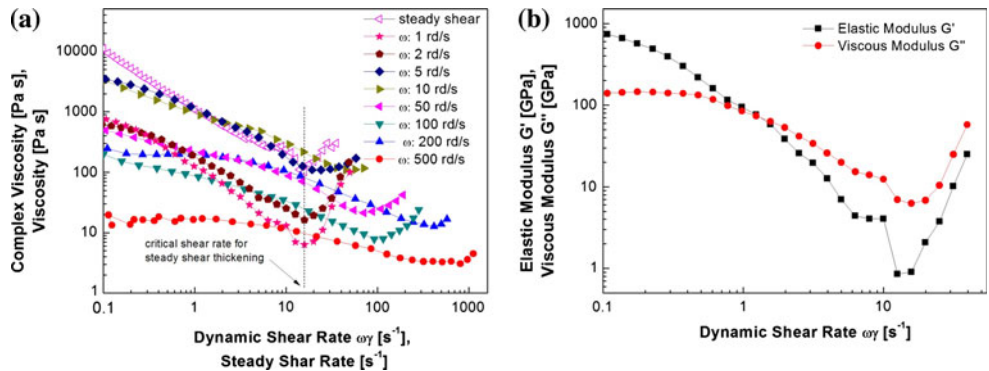


Fig. 8 **a** The dynamic rheological behaviour compared with the steady shear behaviour, using a gap size of 800 μm . **b** Elastic G' and viscous G'' moduli as a function of the maximum shear rate at a constant frequency of 1 rad/s

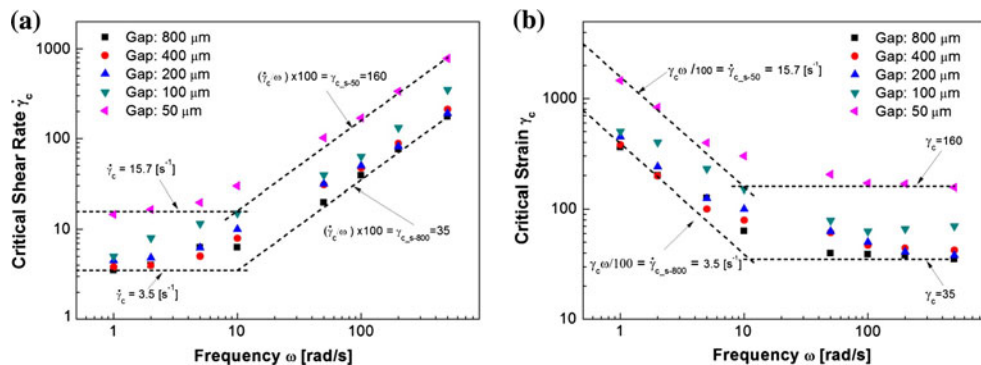
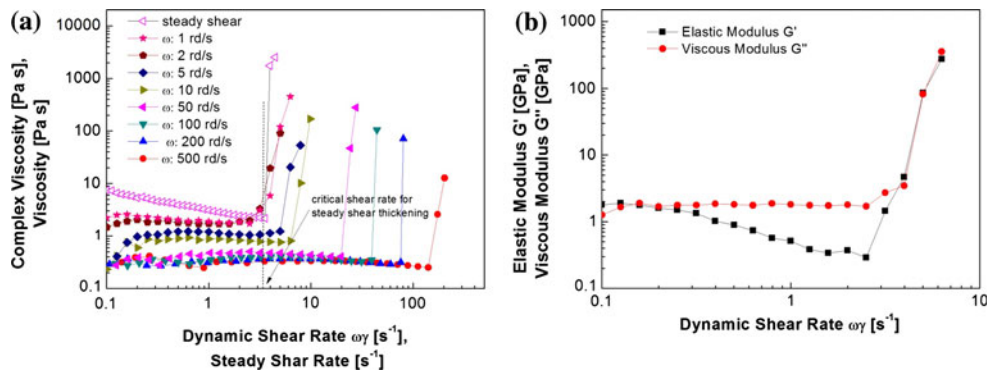


Fig. 9 **a** Critical shear rate and **b** critical strain amplitude, as functions of frequency. The inserted lines $\dot{\gamma}_c = \gamma_c \omega / 100 = 3.5 \text{ s}^{-1}$ and $\dot{\gamma}_c = \gamma_c \omega / 100 = 15.7 \text{ s}^{-1}$ indicate the constant shear rates which equate the steady critical shear rates, $\dot{\gamma}_{c,s=50}$ and $\dot{\gamma}_{c,s=800}$ measured at a gap size of 50 and 800 μm , respectively (cf. Fig. 6). In addition,

$\gamma_c = (\dot{\gamma}_c / \omega) \times 100 = 35$ and $\gamma_c = (\dot{\gamma}_c / \omega) \times 100 = 160$ indicate the constant strains which equate the measured critical strain amplitudes at higher-frequency dynamic oscillatory conditions, $\gamma_{c,d=50}$ and $\gamma_{c,d=800}$, at a gap size of 50 and 800 μm

of the dynamic shear-thickening behaviour can also be well illuminated by the critical strains as a function of the applied frequency (Fig. 9b). Correspondingly, the critical strain for dynamic shear thickening decreases with increasing frequency in the low-frequency range, but finally becomes stable for higher frequencies. This is consistent with the result reported by other researches [4, 5, 11, 12]. However, to accurately interpret the observed data, two factors have to be considered, i.e. the flocculation of particles and the wall-slipping effects.

As mentioned before, the steady rheological behaviour of the polymer dispersion is greatly affected by the micro-sized flocculation of particles when the gap size is small. Such characteristics of the flocculated system are also evidenced by the viscoelastic response of the material under oscillatory motion. As shown in Fig. 7b, when the gap size is relatively small, the elastic modulus G' is nearly one order in magnitude higher than the loss modulus G'' at low strain amplitudes, indicating flocculated gel-like behaviour [4]. With an increase in the strain amplitude, G'

of the material decreases more rapidly than G'' . Accordingly, the material shows shear thinning in the low shear strain regime (Fig. 7a), which has also been observed under steady flow. The random distribution of the flocculation in the dispersion can also explain the poor repeatability of the viscosities measured for small gaps (e.g. Fig. 7a). With an increase in gap sizes, the effect of the flocculation on the initial flow behaviour is much less pronounced and therefore the sample behaves as a liquid. As shown in Fig. 8b, for a gap size of 800 μm , the moduli of the sample are initially low, and the loss modulus G'' quickly dominates the G' during the shearing process. Accordingly, the complex viscosities are relatively stable and much smaller than those measured for smaller gaps (cf. Figs. 7a and 8a).

The effect of geometry-dependent wall slipping (cf. Eq. 1) was also observed under dynamic oscillation, which well explains the higher critical strains measured for smaller gap sizes (Fig. 7). Moreover, it has been postulated that the wall-slipping behaviour is also dependent on the frequency applied during dynamic oscillatory motion [5, 15]. For example, on the basis of Eq. 1, Lee and Wagner [5] correlated the measured strain with the applied frequency. It was indicated that the real strain γ_r can be determined by the shear stress τ and the real viscosity η_r , namely, $\gamma_r = \tau / (\eta_r \omega)$. Substituting this into Eq. 1, the measured strain is

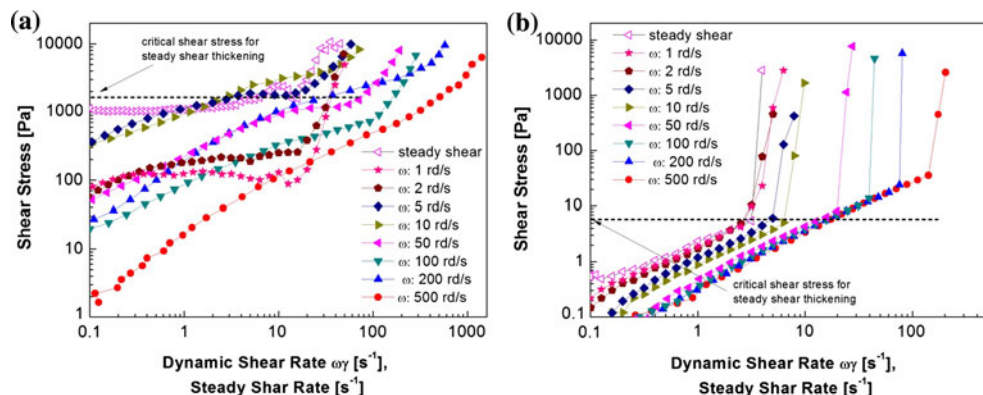
$$\gamma_m = \tau / (\eta_r \omega) + D_s/h \quad (2)$$

According to the assumption that the shear-thickening transition is shear stress controlled, Lee and Wagner [5] further modelled the measured critical strain γ_{m_c} , by

$$\gamma_{m_c} = \tau_c / (\eta_{r_c} \omega) + D_s/h \quad (3)$$

where τ_c is the critical shear stress for the onset of shear thickening, and η_{r_c} is the real viscosity at the shear thickening point. Equation 3 also suggests that the observed minimum strain at high frequencies could be due to the slipping, as $\gamma_{m_c} \approx D_s/h$ when the frequency is high enough [5].

Fig. 10 Shear stress as a function of shear rate (the maximum shear rate for dynamic oscillation) for a gap size of **a** 50 μm , and **b** 800 μm , respectively



To examine the above assumptions, Fig. 10 compares the stress versus shear rate curves obtained at different frequencies. It is observed that the critical shear stresses for the shear-thickening transition are not consistent. Nevertheless, for a large gap, the critical shear stress remains stable within the low frequency range up to 10 rad/s (Fig. 10b). This can be explained by the fact that the flow behaviour of the dispersion becomes stable at larger gap sizes, since it is less affected by the flocculation of the particles. The slight decrease in measured viscosities with higher frequencies gives the hint to the frequency-related wall slipping (Fig. 8a), which may also account for the shifted critical strains within low frequencies regime, as shown in Fig. 9. However, with a further increase in frequency, the critical shear stress increased proportionally (Fig. 10b), indicating the changes in the real critical shear rate.

Therefore, on the basis of the discussions mentioned above, it is known that the dynamic shear thickening occurs only when both the critical shear rate and the minimum oscillatory amplitude are reached simultaneously (cf. Fig. 9), although the measured values of the shear rate and viscosity can be affected by wall slipping, depending on the gap size and the frequency applied.

Discussion on the shear-thickening mechanism

The experimental analysis has shown that the shear-thickening transition occurs only when a critical shear rate is reached, which agrees well with the hydroclusters theory [4, 14, 15]. The theory showed that the onset of shear thickening is driven by the hydrodynamic forces, which is directly proportional to the shear rate [14, 15]. Moreover, according to Bossis and Brady [14], the hydrodynamic stress is proportional to the cube of the larger dimension situated in the plane of shear, which suggests that micro-sized elongated flocculations in the polymer dispersion will contribute to the flow behaviour much more than submicron-sized particles (cf. Fig. 3). Therefore, it is proposed

here that, when the critical shear rate is reached, the shear thickening happens, as hydrodynamic forces are high enough to force the flocculations towards contact along the compressive axis of the shear flow, resulting in a blockage of matrix flow. This can explain the critical shear rates for the shear thickening under steady shear, as well as under low-frequency oscillatory conditions (cf. Fig. 9). However, for oscillation tests at higher frequencies, the critical shear rate could be reached with very small strain amplitudes. In this case, the flocculations might oscillate only around their equilibrium positions rather than aggregated together, due to the small deformations and high frequencies. Hence, a minimum critical strain is also necessary for the onset of shear thickening, as observed under high frequencies oscillatory conditions (cf. Fig. 9).

Finally, it is worthwhile to address the first normal stress difference, an important non-Newtonian characteristic of the fluid. In general, the stresses generated for a simple flow include the shear stress τ_{21} and the normal stresses σ_{11} , σ_{22} and σ_{33} , where the subscripts “1” refers to the flow direction, “2” the normal direction and “3” the vorticity direction (cf. Fig. 4). The normal stresses are customarily written in terms of the first normal stress difference $N_1 \equiv \sigma_{11} - \sigma_{22}$, and the second normal stress difference $N_2 \equiv \sigma_{22} - \sigma_{33}$, which can be measured using the commercial rheometers by determining the total normal force on the stationary plate [20, 22, 23]. In principle, normal stress differences can arise only if there is anisotropy in the microstructure of the suspensions [20]. In particular, according to the Stokesian dynamics simulations and experiments for the concentrated hard-sphere systems, the first normal stress difference would be negative in the shear-thickening regime [21, 22]. In our case, however, it was found that the fluid exhibited large positive first normal stress difference associated with the thickening transition (Fig. 11), suggesting that jamming of particles has occurred [6]. A similar phenomenon was noticed in fumed

colloidal [24] and ferric-oxide suspensions [25]. The nature of this behaviour is still less clear, as the precise measurement of normal stress difference is actually quite difficult [21, 24]. More experiments are still required to reveal the underlying mechanism. Nevertheless, it should be noted that the large normal stress is of great importance for the engineering applications, since it could provide extra loading support in various technical situations.

Conclusions

In this study, the shear thickening behaviour of a polymer suspension was systematically studied under both steady shear and dynamic oscillatory conditions. The following conclusions can be drawn:

1. It was found that the micro-sized flocculation of particles could significantly affect the rheology of the material, depending on the gap size between the plates. Using a small gap size, e.g. 50 μm , the material shows a flocculated, gel-like behaviour, and shear thinning effects are observed under steady flow at lower shear rates, as well as under dynamic oscillatory motion with low strain amplitudes. However, using larger gap sizes, the effects of the micro-sized flocculations are less pronounced at the low shear rates regime, and therefore the viscosity of the fluid is rather low and stable.
2. Under steady flow, shear thickening always occurs when the critical shear rate is reached. However, the measured shear rates can be affected by geometry-dependent wall-slipping phenomena.
3. During dynamic oscillation, the critical strain for shear thickening decreases with an increase in frequency, and it reaches a minimum critical strain for the onset of shear thickening within the high-frequency regime. Moreover, the low-frequency dynamic oscillatory behaviour can be reasonably interpreted in terms of the steady shear behaviour. The critical dynamic shear rate remains stable within the low-frequency regime, which agrees well with the critical shear rate for steady shear thickening.

Acknowledgements The authors are grateful to the Institute for Composite Material (IVW GmbH, Germany) where most of the results were generated. Dr.-Ing L. Chang wishes to thank the Alexander von Humboldt-Foundation for his research fellowship at IVW.

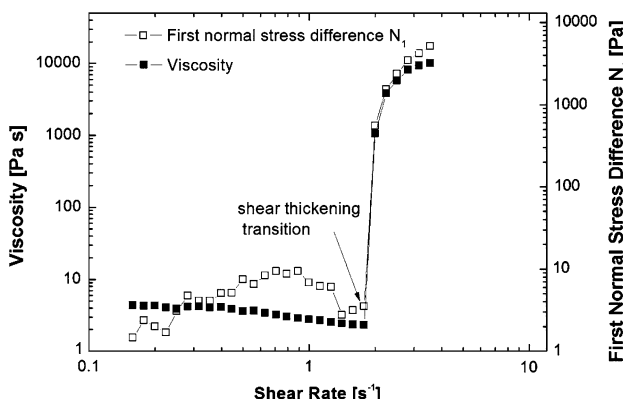


Fig. 11 Positive first normal stress differences corresponding to the steady shear thickening measured for a gap size of 800 μm

References

1. Hoffman RL (1972) Trans Soc Rheol 16:155
2. Hoffman RL (1974) J Colloid Interface Sci 46:491

3. Barnes HA (1997) *J Non-Newton Fluid Mech* 70:1
4. Raghavan SR, Khan SA (1997) *J Colloid Interface Sci* 185:57
5. Lee YS, Wagner NJ (2003) *Rheol Acta* 142:199
6. Fall A, Huang N, Bertrand F, Ovarlez G, Bonn D (2008) *Phys Rev Lett* 100:018301
7. Helber R, Doncker F, Bung R (1990) *J Sound Vib* 138:47
8. Lee YS, Wetzel ED, Wagner NJ (2003) *J Mater Sci* 38:2825. doi:[10.1023/A:1024424200221](https://doi.org/10.1023/A:1024424200221)
9. Fischer C, Braun SA, Bourban PE, Michaud C, Plummer C, Manson J (2006) *Smart Mater Struct* 15:1467
10. Vermant J, Solomon MJ (2005) *J Phys Condens Matter* 17:187
11. Doraiswamy D, Mujumdar AN, Tsao I, Beris AN, Danforth SC, Metzner AB (1991) *J Rheol* 35:647
12. Laun HM, Bung R, Schmidt F (1991) *J Rheol* 35:999
13. Bender JW, Wagner NJ (1995) *J Colloid Interface Sci* 172:171
14. Bossis G, Brady JF (1989) *J Chem Phys* 91:1866
15. Boersma WH, Laven J, Stein HN (1992) *J Colloid Interface Sci* 149:10
16. Farr RS, Melrose JR, Ball RC (1997) *Phys Rev E* 55:7203
17. O'brien VT, Mackay ME (2000) *Langmuir* 16:7931
18. Holmes CB, Fuchs M, Cates ME (2003) *Europhys Lett* 63:240
19. Brown E, Jaeger HM (2009) *Phys Rev Lett* 103:086001
20. Singh A, Nott PR (2003) *J Fluid Mech* 490:293
21. Singh A, Nott PR (2000) *J Fluid Mech* 412:279
22. Laun HM (1994) *J Non-Newton Fluid Mech* 54:87
23. Jomha AI, Reynolds PA (1993) *Rheol Acta* 32:457
24. Negi AS, Osuji CO (2009) *Rheol Acta* 48:871
25. Kanai H, Amari T (1995) *Rheol Acta* 34:303